Predicting Effective Connectivity From Resting-State Networks in Healthy Elderly and Patients With Prodromal Alzheimer's Disease

Susanne Neufang,[1]* Atae Akhrif,[1] Valentin Riedl,[2] Hans Förstl,[3] Alexander Kurz,[3] Claus Zimmer,[1] Christian Sorg,[1,3] and Afra M. Wohlschläger[1,2]

[1]*Department of Neuroradiology, Klinikum Rechts der Isar, Technical University Munich, Ismaningerstrasse 22, 81675 Munich, Germany*
[2]*Department of Neurology, Klinikum Rechts der Isar, Technical University Munich, Ismaningerstrasse 22, 81675 Munich, Germany*
[3]*Department of Psychiatry, Klinikum Rechts der Isar, Technical University Munich, Ismaningerstrasse 22, 81675 Munich, Germany*

Abstract: Using functional neuroimaging techniques two aspects of functional integration in the human brain have been investigated, functional connectivity and effective connectivity. In this study we examined both connectivity types in parallel within an executive attention network during rest and while performing an attention task. We analyzed the predictive value of resting-state functional connectivity on task-induced effective connectivity in patients with prodromal Alzheimer's disease (AD) and healthy elderly. We found that in healthy elderly, functional connectivity was a significant predictor for effective connectivity, however, it was frequency-specific. Effective top-down connectivity emerging from prefrontal areas was related with higher frequencies of functional connectivity (e.g., 0.08–0.15 Hz), in contrast to effective bottom-up connectivity going to prefrontal areas, which was related to lower frequencies of functional connectivity (e.g., 0.001–0.03 Hz). In patients, the prediction of effective connectivity by functional connectivity was disturbed. We conclude that functional connectivity and effective connectivity are interrelated in healthy brains but this relationship is aberrant in very early AD. *Hum Brain Mapp 35:954–963, 2014.* © 2013 Wiley Periodicals, Inc.

Key words: effective connectivity; resting-state functional connectivity; executive attention network; prodromal Alzheimer's disease

Additional Supporting Information may be found in the online version of this article.

Contract grant sponsor: German Federal Ministry of Education and Research; Contract grant number: 01EV0710; Contract grant sponsor: Kommission für Klinische Forschung of the university hospital Klinikum Rechts der Isar; Contract grant number: C21-09/8762753; Contract grant sponsor: Alzheimer Forschung Initiative (AFI); Contract grant numbers: 08860, 8762754.

*Correspondence to: Susanne Neufang, Department of Neuroradiology, Klinikum Rechts der Isar, Technische Universität Munich, Ismaningerstrasse 22, 81675 Munich, Germany.
E-mail: Neufang@lrz.tu-muenchen.de

Received for publication 31 January 2012; Revised 12 September 2012; Accepted 22 October 2012

DOI: 10.1002/hbm.22226
Published online 10 January 2013 in Wiley Online Library (wileyonlinelibrary.com).

© 2013 Wiley Periodicals, Inc.

INTRODUCTION

In the recent years brain connectivity has been studied via numerous methods and with regard to different modalities. The most commonly used MRI-based methods to address brain connectivity were (i) fractional anisotropy (FA) revealed from Diffusion Tensor Imaging (DTI) for structural connectivity (for review see Mori and Zhang, 2006), (ii) resting state networks (RSNs) determined from resting-state fMRI (rs-fMRI) for functional connectivity (for review see Van den Heuvel and Hulshoff Pol, 2010), and (ii) Dynamic Causal Modeling (DCM) determined from task-fMRI for effective connectivity (for review see Stephan and Friston, 2010). For a better understanding of the nature of brain connectivity, measures of the different modalities have been combined.

With regard to the relation between RSNs and structural connectivity, for example, it is widely believed that RSNs are more or less based on fiber architecture. As RSNs indicate neuronal connectivity between distant brain regions, "these regions must use neuronal connections to carry the associated information flow. To allow for such communication between nodes of brain networks there must be a white matter fiber path connecting them. This pathway does not have to be direct, but nevertheless one expects that functional connectivity must in some manner be dependent on the strength of the relevant anatomical neuronal connection" [Damoiseaux and Greicius, 2009; Skudlarski et al., 2008]. Using seed regions from functional connectivity maps of the default mode network (DMN) in DTI analyses, Greicius et al. [2009] found strong fiber tracts between network regions concluding that RSNs "reflect" the anatomical fiber architecture [Greicius et al., 2009]. A close relation has been reported for the DMN [Greicius et al., 2009; Skudlarski et al., 2008], as well as for the executive/dorsal attention network [Fox et al., 2009; Ystad et al., 2011]. In the diagnostic context, this methodological approach has shown great benefit: For example, Wee et al. [2011] applied a classification algorithm on combined DTI and rs-fMRI data of healthy elderly and individuals at risk for amnestic mild cognitive impairment (aMCI). They were able to improve classification accuracy significantly compared to classification results from a unimodal approach [Wee et al., 2011].

To date the relation between effective and structural connectivity has not been addressed very often. Findings were rather theoretical than empirically proven. For instance, in the theory of effective dysconnection in schizophrenia [Stephan et al., 2009] an indirect influence of effective connectivity on fiber architecture has been described in terms of impairments in effective connectivity (dysconnectivity) might lead to alterations in the fiber architecture over the course of time. The assumed mechanism is that effective connectivity reflects synaptic plasticity and alterations in synaptic activity might influence fiber architecture [Stephan et al., 2009].

With regard to functional and effective connectivity, both measures characterize functional integration within the human brain. However, while functional connectivity describes statistical dependencies between data effective connectivity rests on a mechanistic model of causal effects that generated the data [Stephan et al., 2010]. In short, functional connectivity between regions within RSNs is determined by spatially coherent, spontaneous fluctuation in the blood oxygen level-dependent signal and is made up of regional patterns commonly involved in functions such as sensory, attention, or default mode processing. RSNs are networks identified by a data-driven approach (independent component analysis, ICA). In addition, previous studies investigating RSNs have used region-of-interest (ROI)-based analyses [Fox et al., 2005; Salvador et al., 2005; Wang et al., 2006]. The signal time course of a selected ROIs, e.g., the local maxima of RSN regions, are correlated with remaining network areas resulting in pairwise functional connectivity coefficients. Effective connectivity, in general, describes the causal influence that neural units exert over another [Friston, 1994], specified "in the simplest possible circuit diagram that would replicate the observed timing relationships between recorded neurons" [Aertsen and Preiβl, 1999]. In the DCM procedure models are *a priori* defined and compared with regard to the best fit (or better "highest evidence," a combination between fit and complexity, Stephan et al., 2010). Two types of connectivity are specified (i) endogenous connectivity as the fixed connectivity among the network regions in the absence of input, and (ii) modulatory input: the change in connectivity induced by the input of exogenous influences (e.g., psychological stimulation via an experimental paradigm). Resulting connectivity parameters are pair-wise coefficients describing the influence from one region to a second. The empirical combination of effective and functional connectivity, so far, mainly consisted of an exchange of methods, such as determining RSNs from task-fMRI data [Ozaki et al., 2011] and applying effective connectivity parameters from rs-fMRI data [Granger causality: Liao et al., 2010; a DCM-like procedure: Havlicek et al., 2011]. The main idea of these studies was to better characterize the functional architecture of RSNs and reveal possible dynamical changes within the same.

However, the questions whether functional connectivity reflects effective connectivity or better, whether rs-fMRI parameters might predict network dynamics during task-fMRI have not been addressed in these studies. Especially with regard to the clinical benefit of rs-fMRI, this subject might be interesting (rs-fMRI as a diagnostic tool for cognitive state or psychiatric diseases?).

In this study we examined the relation between functional connectivity from rs-fMRI and effective connectivity from task-fMRI within an executive/dorsal attention network. We chose this network as it has been robustly found in numerous studies using both fMRI techniques [for reviews see Van Dijk et al., 2010; Rossi et al., 2009]. To address the clinical question we analyzed not only data of healthy subjects ($n = 16$) but also psychiatric patients suffering from aMCI ($n = 24$). In aMCI and Alzheimer's

TABLE I. Sample description

	HC ($n = 16$)	pAD ($n = 15$)	Analysis
Age [years]	68.1 ± 3.8	68.5 ± 6.6	$t_{(2,29)} = -0.24$, n. s.
Sex [male/female]	9 / 7	6/9	$\aleph^2 = 0.82$, n. s.
education [</> 12 years]	9 / 7	7/8	$\aleph^2 = 0.54$, n. s.
CDR (sum of boxes)	–	2.6 ± 0.9	
MMSE	29.6 ± 0.5	27.4 ± 1	$t_{(2,29)} = 7.8$, $P < 0.01$
CERAD [delayed recall- n^o of items]	7.4 ± 1.3	3.7 ± 2.3	$t_{(2,29)} = 5.6$, $P < 0.01$

Mean and standard deviations of demographical and neuropsychological parameters. Data are presented as Mean ± Standard Deviation. MMSE, Mini-Mental State Exam; CERAD, consortium to establish a registry for Alzheimer's Disease; CDR, Clinical Dementia Rating.

disease (AD), attention deficits have been associated with a frontal disconnection as described by Perry and Hodges [1999]. In a recent study of our lab, we could furthermore show, that effective connectivity, emerging from parietal areas and going to frontal and cingular regions was also reduced, hinting towards not only a frontal but also a parietal disconnection in the context of AD [Neufang et al., 2011]. In addition, numerous studies showed altered functional connectivity within the dorsal/executive attention network in aMCI patients [e.g., Sorg et al., 2007] as well as in AD patients [i.e., Wang et al., 2006].

To be able to directly combine both connectivity parameters in regression models, we determined functional connectivity from RSNs using the ROI-based partial coherence (pC) analysis. We raised the questions (i) whether functional connectivity from rs-fMRI could predict the strength of effective connectivity during cognitive processing and (ii) if so, would it also be possible in affected brains such as in aMCI patients. On the basis of the introduced findings of a strong connection between RSNs and fiber architecture [Damoiseaux and Greicius, 2009; Greicius et al., 2009; Skudlarski et al., 2008; Wee et al., 2011; Ystad et al., 2011] and the assumed relation between effective connectivity and structural connectivity [Ozaki et al., 2011; Liao et al., 2010; Havlicek et al., 2011; Stephan et al., 2009] we hypothesized to find a significant correlation between RSNs and DCM estimates. Inferring from our previous findings [Neufang et al., 2011] we expected aMCI-related alterations, if present, more prominent within fronto-parietal connections than those associated with the cingulate cortex.

MATERIALS AND METHODS

Subjects

Sixteen healthy controls (HC) (6 females, aged from 63 to 73 years) and twenty four patients diagnosed with amnestic mild cognitive impairment (aMCI) participated in the study. Fifteen patients developed AD-related dementia in annual clinical follow-up evaluations within two years after this examination (NINCDS-ADRDA criteria for AD) [McKhann et al., 1984]. Data analysis of the clinical group was restricted to these 15 participants (9 females, aged from 58 to 73 years), so the study patients can be defined as prodromal Alzheimer's disease (pAD) patients. HC subjects and pAD patients were matched for age, education and gender (see Table I)

Patients were recruited from the Memory Clinic of the Department of Psychiatry, Technical University Munich, Germany, controls by word-to-mouth advertising. Examination of every subject included medical history, neurological examination, neuropsychological assessment (CERAD battery, Consortium to Establish a Registry for AD [Morris et al., 1989], informant interview (patients only), and structural MRI. Patients met criteria for aMCI [Gauthier et al., 2006] which contained reported and neuropsychologically assessed memory impairments, largely intact activities of daily living, and excluded dementia (see Table I).

Six control subjects and three patients were treated for hypercholesterolemia (statins). None of the subjects had diabetes mellitus and none received psychotropic medication, especially cholinesterase inhibitors. Further exclusion criteria for entry into the study were other neurological, psychiatric, and systemic diseases (i.e., stroke, depression, alcoholism, and hypertension) anytime before or at the examination date, or clinically remarkable MRI (e.g., stroke lesions). The study was approved by the Medical Ethics Committee of the Faculty of Medicine, Technical University Munich, Germany. All participants provided informed consent in accordance with the Human Research Committee guidelines of the Klinikum Rechts der Isar, Technical University Munich.

fMRI Paradigms

Resting-state fMRI

All subjects underwent four minutes of resting-state scan. Subjects were instructed simply to keep their eyes closed, not to think of anything in particular, and not to fall asleep.

Task fMRI

The task-fMRI session included an attention and a memory task, which followed the resting-state scan. In this study, we will focus on the attentional paradigm and the resting-state scan; the memory task will not be part of this study.

In the MR scanner subjects performed the Attention Network Task [ANT, Fan et al., 2005], which measured the three different attentional functions alertness, spatial orienting and conflict processing. Network-specific stimulation was realized via a variation of cue—target combinations covering the four cue conditions "no cue," "central cue," "double cue," and "spatial cue" as well as the three target conditions "congruent targets," "incongruent targets," and "neutral targets.". The cues consisted of one or two asterisks presented either in the center of the screen (central, double), above the central position (spatial_up), or below it (spatial_down). Cues without spatial information such as the central cue and the double cue were implemented in the task in order to provoke an alerting reaction in the subject (alertness: central cue> no cue, double cue > no cue). Cues with spatial information indicated the upcoming target position (under or above the screen center) and intended to initiate an orienting of the attentional focus onto the indicated position (orienting: spatial_up cue>no cue, spatial_down cue>no cue). The congruent and incongruent target stimuli were composed of a row of five horizontal black arrows, with the arrowheads pointing either leftward or rightward. To introduce a conflict resolution component, the central arrow was "flanked" on either side by two arrows in the same direction (congruent condition) or in the opposite direction (incongruent condition), effecting a conflict situation the way that the participants had to focus on the target arrow while ignoring the context arrows (conflict: incongruent> congruent targets). Neutral targets were a single arrow pointing either to the right or the left side. The participants' task was to identify the direction of the centrally presented arrow by pressing a button with the index finger of the right hand for the left direction and a button with the middle finger of the right hand for the right direction (see also Supporting Information, Fig. S1).

Although three different networks were stimulated in this paradigm, we focus on the conflict network in this study. Thus, the attention networks alerting and orienting will not be considered. With regard to the conflict network, we expect an increase in brain activation within a cingulo-fronto-parietal network during the processing of incongruent targets compared to congruent trials.

The paradigm was presented as an event-related design with cue-target intervals varying from 500 ms to 12 s (average interval of 3 s) and intertarget intervals between 3 and 20 s (mean interval was 8 s). Cues were presented for 200 ms, targets were shown for 2,000 ms. Totally, 128 trials were presented (56 congruent/incongruent trials, 16 neutral; 20 trials of each cue, 48 "no cue" trials) within one single run; the scanning time was about 18 min.

Imaging Data Acquisition

Imaging was performed on a 1.5 T Siemens Symphony system. Structural images were acquired using an isotropic T1-weighted MPRAGE (magnetization-prepared rapid acquisition gradient echo) sequence with the following parameters: TR = 1,500 ms, TE = 3.93 ms, TI = 760 ms, flip angle = 5°; FOV = 256 mm^2; matrix = 256 × 256; 160 slices, slice thickness 1 mm, voxel size = 1 × 1 × 1 mm^3).

Functional data were collected by using a gradient echo EPI sequence (EPI) with the following parameters: TR (repetition time) = 3,000 ms, TE (echo time) = 50 ms, TI (inversion time) = 2,630 ms, 33 4-mm-thick axial slices with a 0.4-mm gap, matrix size = 64 × 64, field of view (FoV) = 200 mm^2, flip angle = 90°. The first three volumes were discarded to allow for T1 equilibration effects. For each subject, 360 functional whole-brain images were acquired in the task session, 80 volumes in the resting-state scan.

TABLE II. fMRI activations patterns in resting state fMRI and task fMRI, reported are coordinates of the local maxima (*x*,*y*,*z*) and statistical power (*Z*-score)

Region of interest	Resting-state fMRI				Task-fMRI			
	X	*y*	*z*	*Z*	*x*	*y*	*z*	*Z*
rMFG	54	9	45	5.2	54	6	39	4.7
lSPG	−63	−30	24	6.2	−36	−48	42	4.7
rSPG	18	−66	54	5.7	21	−72	51	4.6
rRZCa	6	18	33	4.1	6	21	42	3.8

Z-values are reported FWE-corrected for multiple comparisons. rMFG, right middle frontal gyrus; lSPG, left superior parietal gyrus; rSPG, right superior parietal gyrus; rRCZa, right rostral cingulate zone, part anterior. Coordinates were reported in MNI-space.

fMRI Data Analysis

Data preprocessing and statistical analyses were performed using the Statistical Parametric Mapping (SPM) software (http//www.fil.ion.ucl.ac.uk/spm). Data of both, resting-state scan and task measurements, were motion-corrected, coregistered onto the individual anatomical T1, spatially normalized into the stereotactic space of the Montreal Neurological Institute (MNI) (T1 template, 2 × 2 × 2 mm voxel resolution) and spatially smoothed with an 8 × 8 × 8 mm Gaussian kernel full-width-half-maximum to accommodate inter-subject anatomical variability (for more information see Supporting Information).

Functional connectivity-partial coherence analysis

In this study, we focused on ROI-based pC analyses within the executive/dorsal attention network. All preceding analyses including the identification of RSNs using ICA and their statistical analyses have been described in an earlier study [Sorg et al., 2007, for details see also Supporting Information]. For our ROI-analysis we used the significantly coactivated network regions of the executive/

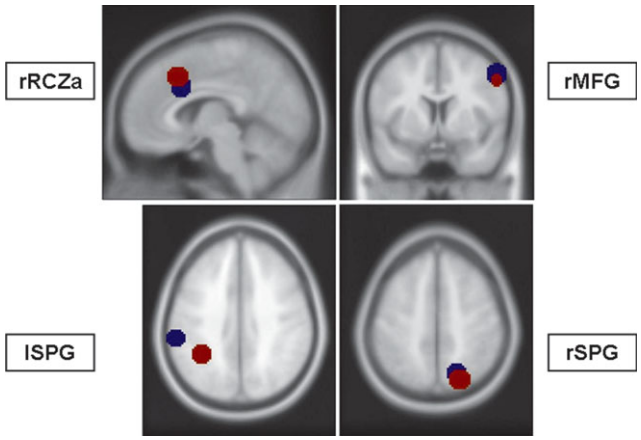

Figure 1.
Regions of interest of the cingulo-fronto-parietal network. Blue dots represent regions for effective connectivity; red dots indicate the regions for functional connectivity analyses.

dorsal attention network (see Table II and Fig. 1, red dots; Supporting Information Fig. S2), located within the right and left superior parietal gyri, the right middle frontal gyrus as well as within the right anterior cingulate cortex. We constructed spherical regions ($r = 10$ mm) around the peak voxel of the significant clusters within these ROIs and extracted the voxelwise BOLD time courses (tc). For each tc the first eigenvector was derived with singular value decomposition yielding the most prominent proportion in the BOLD signal. The signal from global gray matter, CSF and deep white matter was removed from the tc through linear regression in the time domain [Fox et al., 2009]. A *Z*-transformation of the resulting time courses was applied to yield normal distribution. Using these tcs, pair-wise connectivity parameters for right fronto-parietal connections, fronto-cingular, and inter-parietal connections were determined. We chose the methodological approach of pC [e.g., Kaminski, 2006; Salvador et al., 2005; Sato et al., 2009; Sun et al., 2004], as in contrast to simple time series correlations, pC is a multivariate approach, treating fMRI data as a set of voxel changing their state in time [for discussion see Sun et al., 2004, Appendix A]. Mathematically, pC estimations are repeated for each region in the context of inter-regional relations:

In the frequency domain a function analogous to correlation is coherence *K*. *K* compares common behavior of components of signals $\times$ and y at different frequencies f. It is a function of the power spectral density (PSD) P_{xx} and P_{yy} and the cross power spectral density (CPSD)P_{xy}

$$K(x,y,f) = \frac{P_{xy}(f)}{\sqrt{P_{xx}(f)P_{yy}(f)}}$$

The modulus of ordinary coherence takes values in the [0, 1] range. It describes the amount of in-phase components in both signals at frequency f (0 indicates no relation). When a system consists of more than two channels there is always the possibility that some channels may influence others indirectly which results in a significant amount of coherence between those channels although they are not directly related to each other. Functions which help to decompose complex relations between signals and describe only direct ones are called partial functions [Jenkins and Watts, 1998]. All relations which can be explained by linear combinations of other data channels will not be shown by this measure.

$$C_{xy}(f) = \frac{M_{xy}(f)}{M_{xx}(f)M_{yy}(f)}$$

Its modulus takes values within the [0, 1] range similar to the ordinary coherence, but it is nonzero only when the relation between x and y is direct. M_{xy} is a minor of the spectral matrix $\boldsymbol{P}$ with i-th row and the j-th column removed.

$$P(f) = \begin{bmatrix} P_{11} & P_{12} & \cdots & P_{1n} \\ P_{21} & P_{22} & \cdots & P_{2n} \\ \vdots & \vdots & \ddots & \vdots \\ P_{n1} & P_{n2} & \cdots & P_{nn} \end{bmatrix}$$

To examine coherence profiles between the ROIs we determined pC coefficients for each pair of ROIs, obtaining 4 x 4 coherence matrix. Because of the used sampling rate of TR = 3 s, the tcs had a bandwidth of 0.001–0.15 Hz. For statistical analysis, frequencies were summarized according to Garrity et al. [2007] into the following four frequency bins (fb1 = 0.001–0.03 Hz, fb2 = 0.04–0.08 Hz, fb3 = 0.09–0.13 Hz, fb4 = 0.13–0.15 Hz).

Effective connectivity-dynamic causal modeling

Like in the analyses of pC coefficients from rs-fMRI, effective connectivity analyses were based on fMRI-data processing (e.g., specification of condition-specific contrasts on the single subject level, group analyses using one sample *t*-Tests and group comparisons), which has been reported in an earlier study (for a detailed description see Neufang et al., 2011, and Supporting Information). For the DCM, we used DCM10 as implemented in the SPM8 software. The regions, which entered the DCM analysis were conflict-associated activations in the right middle frontal gyrus (MFG), bilaterally in the superior parietal gyrus (SPG) and the right anterior cingulate cortex, more precisely in the rostral cingulate zone, part anterior (RCZa), revealed from fMRI analyses (see Table II, and Supporting Information). Subjects entered the analysis if the subjects-specific maxima were located (i) within a radius of 10 mm around the group maxima and (ii) within the same gyrus (see Table II and Fig. 1, blue dots). Regional time series were extracted as the

first eigenvariate of all activated voxel within a 10 mm radius around the subject-specific maximum.

Connectivity parameters were estimated within the identified model of highest evidence (for model selection see Neufang et al., 2011 and Supporting Information) including bidirectional endogenous connectivity (eC) between the right MFG and parietal areas (rMFG→rSPG, rMFG→lSPG, rSPG→rMFG, lSPG→rMFG), interparietal connections (lSPG→rSPG, rSPG→lSPG), and unilateral connectivity from the right MFG to the right RCZa (rMFG→rRCZa). Modulatory input (mI), the change of connectivity strength due to external stimulation, was modeled for the connections from the right MFG to parietal areas and the right RCZa assuming a direct, linear, frontal top-down modulation. Estimates for eC and mI were then calculated.

Statistical Analysis

To reveal the relation between both connectivity parameters, we specified regression models using frequency-specific pC coefficients as independent variables and either eC or mI as dependent variables. To compare regression coefficients between groups' regression coefficients were transformed with the Fisher *Z*-transform and compared in relation to the sample size. The two effective connectivity parameters yielded 10 connectivity variables (7 eC and 3 mI); combined with four frequency-specific pC coefficients per connection, we specified 40 regression models. Resulting regression models were:

- eC (rMFG→rRCZa) * pC (rMFG↔rRCZa$_{fb1}$), . . ., pC (rMFG↔rRCZa$_{fb4}$)
- eC (rMFG→rSPG) * pC (rMFG↔rSPG$_{fb1}$), . . ., pC (rMFG↔rSPG$_{fb4}$)
- eC (rMFG→lSPG) * pC (rMFG↔lSPG$_{fb1}$), . . ., pC (rMFG↔lSPG$_{fb4}$)
- eC (lSPG→rMFG) * pC (rMFG↔lSPG$_{fb1}$), . . ., pC (rMFG↔lSPG$_{fb4}$)
- eC (rSPG→rMFG) * pC (rMFG↔rSPG$_{fb1}$), . . ., pC (rMFG↔rSPG$_{fb4}$)
- eC (rSPG→lSPG) * pC (rSPG↔lSPG$_{fb1}$), . . ., pC (rSPG↔lSPG$_{fb4}$)
- eC (lSPG→rSPG) * pC (rSPG↔lSPG$_{fb1}$), . . ., pC (rSPG↔lSPG$_{fb4}$)
- mI (rMFG→rRCZa) * pC (rMFG↔rRCZa$_{fb1}$), . . ., pC (rMFG↔rRCZa$_{fb4}$)
- mI (rMFG→rSPG) * pC (rMFG↔rSPG$_{fb1}$), . . ., pC (rMFG↔rSPG$_{fb4}$)
- mI (rMFG→lSPG) * pC (rMFG↔lSPG$_{fb1}$), . . ., pC (rMFG↔lSPG$_{fb4}$)

As each of the 10 effective connectivity parameter entered into 4 regression models (for each frequency band), we used FDR-correction (Benjamini and Hochberg, 1995) to correct for 40 tests.

RESULTS

Predicting Task-Induced Effective Connectivity Based on Resting-State Coherence in HC Subjects

As hypothesized, we found a significant relation between functional connectivity from rs-fMRI and effective connectivity from task-fMRI within a cingulo-fronto-parietal network. By correlating pC coefficients and eC parameters we found significant associations bidirectional between the right MFG and the right SPG (ec_rMFG→rSPG*rMFG↔rSPG, eC_rSPG→rMFG*rMFG↔rSPG), from the right MFG to the right RCZa (eC_rMFG→rRCZa*rMFG↔ rRCZa) and to the left SPG (eC_rMFG→lSPG*rMFG↔lSPG), as well as from the left SPG to the right SPG (eC_lSPG→rSPG*lSPG↔ rSPG). With regard to the relation between mI estimates and pC coefficients we found a significant correlation in the connection from the right MFG to the right RCZa (mI_rMFG→rRCZa*rMFG↔rRCZa) (see Table III).

Interestingly, correlations between eC / mI estimates and pC coefficients systematically varied between top-down and bottom-up connections: whereas (top-down) connectivity emerging from the right MFG correlated with pC coefficients in bins of high frequencies (fb3 and fb4), (bottom-up) connections going to the right MFG and interparietal connections correlated with pC coefficients in the lowest frequency bin (fb1) (Table III, Fig. 2).

Impaired Relation Between Task-Induced Effective Connectivity and Resting-State Coherence in pAD Patients

In the pAD group, there was no significant correlation between eC/mI estimates and pC coefficients, neither in these bins, where HC controls showed a significant relation nor in differing frequency ranges. The statistical comparison between connectivity parameters in those connections, identified as significantly correlating in the HC group, revealed significant group differences between regression coefficients in all but one of the connections: whereas in the HC group eC/mI estimates were significantly correlated with pC coherence, pAD patients showed either no relation between both parameters or a weak relation in the opposite direction (see Table III, Fig. 3). In the connectivity emerging from the right MFG to the right SPG; however, pAD patients showed a weaker, but not significantly impaired relation.

DISCUSSION

In this study, we examined the relation between functional connectivity from rs-fMRI and effective connectivity from task-fMRI. We raised the questions (i) whether resting-state connectivity could predict the strength of effective connectivity during cognitive processing and (ii) if so,

TABLE III. Frequency bins of significant correlation between partial coherence (pC) coefficients and DCM estimates of endogenous connections (eC)

Connectivity	Fb [Hz]	eC	pC	Beta	*P*
Top-down					
eC_rMFG → rRCZa	fb3 (0.08–0.13)	HC: .02 ± .10 pAD: .01 ± .07	HC: .55 ± .09 pAD: .61 ± .09	HC: .62, $P < 0.05$ pAD: -.08, n. s.	$P < 0.05$*
mI_rMFG → rRCZa	fb3 (0.08–0.13)	HC: -.01 ± .20 pAD: .06 ± .17	HC: .61 ± .09 pAD: .54 ± .09	HC: -.63, $P < 0.05$ pAD: .03, n. s.	$P < 0.05$*
eC_rMFG → lSPG	fb3 (0.08–0.13)	HC: .06 ± .14 pAD: .04 ± .12	HC: .62 ± .10 pAD: .58 ± .12	HC: -.53, $P < 0.05$ pAD: .16, n. s.	$P < 0.05$*
eC_rMFG → rSPG	fb4 (0.13–0.15)	HC: .05 ± .23 pAD: .03 ± .19	HC: .14± .09 pAD: .13 ± .06	HC: .53, p<.05 pAD: .33, n. s.	n. s.
mI_rMFG → lSPG		No significant correlation in any frequency bin			
mI_rMFG → rSPG		No significant correlation in any frequency bin			
Bottom-up					
eC_rSPG → rMFG	fb1 (< .03)	HC: .13 ± .15 pAD: .14 ± .11	HC: .17 ± .10 pAD: .23 ± .19	HC: .59, $P < 0.05$, pAD: -.27, n. s.	$P < 0.05$*
eC_lSPG → rSPG	fb1 (< .03)	HC: .06 ± .14 pAD: .06 ± .19	HC: .13 ± .09 pAD: .11 ± .07	HC: -.62, $P = 0.01$ pAD: .25, n. s.	$P < 0.05$*
eC_rSPG → lSPG		no significant correlation in any frequency bin			
eC_lSPG → rMFG		no significant correlation in any frequency bin			

*$P < 0.05$, FDR-corrected for 40 tests; rMFG, right middle frontal gyrus; lSPG, left superior parietal gyrus; rSPG, right superior parietal gyrus; rRCZa, right rostral cingulate zone, part anterior; HC, healthy controls, pAD, prodromal Alzheimer's Disease.

was this also the case in clinical populations such as pAD patients.

We found, that resting-state functional connectivity was significantly related to task-induced effective connectivity in healthy subjects. This relation was valid for several connections within the examined cingulo-fronto-parietal network. On the basis of our findings, we can say, that the relation (i) was frequency-specific and (ii) disrupted in pAD patients.

With regard to the role of frequencies in rs-fMRI, low frequency BOLD signal fluctuations have been mainly described between 0.01 and 0.08 Hz [Salvador et al., 2008] or <0.1 Hz [Biswal et al., 1997], and also higher frequency bands (up to 0.16 Hz) have been identified as RSN-relevant [Niazy et al., 2011]. These frequency ranges seemed to be both, independent of the used functional connectivity measure [small world, Achard et al., 2006; Supekar et al., 2009, 2008; wavelet-based networks parameters, Ginestet and Simmons, 2011; resting state networks, Lagioia et al., 2010] and valid for different age groups [infant brain, Smyser et al., 2010; children and young adults, Supekar et al., 2009; adolescents, Lagioia et al., 2010; elderly, Supekar et al., 2008]. Furthermore, some studies report network-specific frequency ranges, for example Smyser et al. [2010] found highest signal peaks within the sensori-motor cortex at 0.02–0.04 Hz, in contrast to much broader range of 0.01–0.05 Hz in visual networks. For attention networks, however, no frequencies have yet been reported. We found, that bottom-up connections (from parietal to frontal regions as well as interparietal connections) were associated with frequencies within the rs-fMRI frequency range. In our study, these frequencies might reflect the task-induced spatial processing of the direction judgement from the task instruction and cue-based attentional orienting. In contrast, top-down connectivity was associated with frequencies, higher than the described (>0.08 Hz), which might be interpreted as the reflection of an active, more intensive cognitive processing compared with resting brain activities. Based on the findings from EEG, these interpretation seemed plausible, however, a systematical analysis of frequency bands in fMRI lacks until today.

In pAD patients, in contrast, the relation between functional connectivity and effective connectivity was more

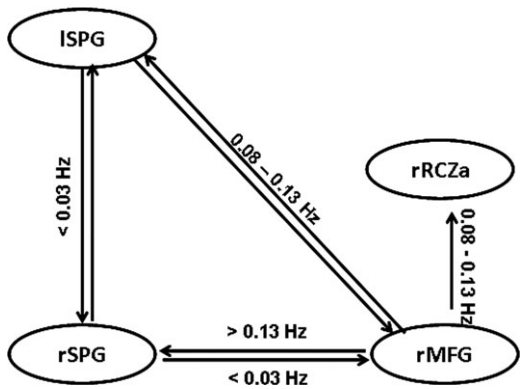

Figure 2.

Sketch of four-area network. Circles represent the structures, the arrows the modelled pair-wise connection. Arrows are labeled with these frequency ranges, in which functional connectivity significantly predicts effective connectivity in healthy control subjects.

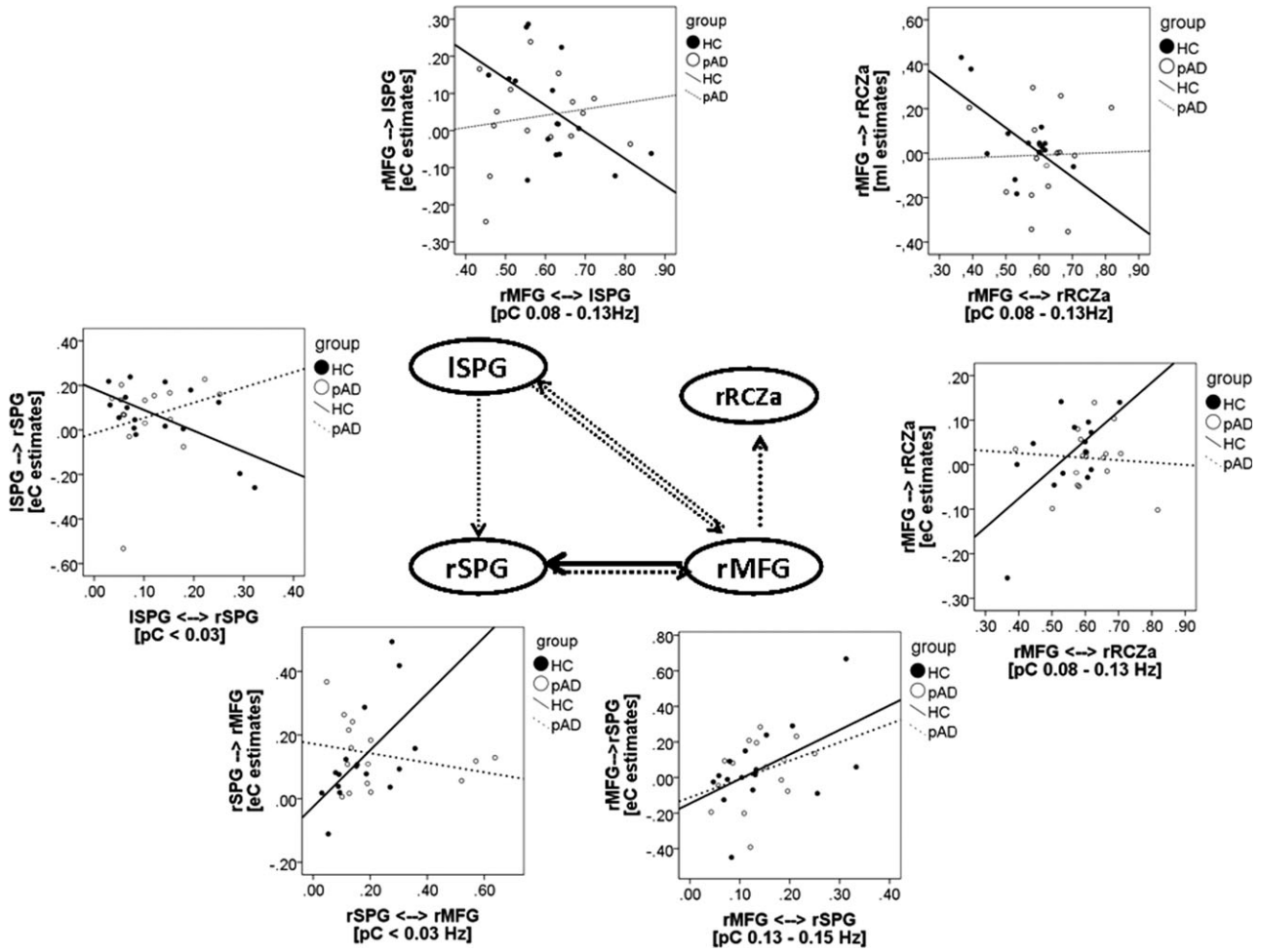

Figure 3.

Sketch of the four-area network. Circles represent the structures, the arrows the modelled pair-wise connection. The black solid arrows mark the connection in which functional connectivity predicted effective connectivity in pAD patients, dotted arrows indicate the connections, where functional connectivity did not predict effective connectivity in pAD patients. The scatter plots show group-specific correlations for these connections. Dotted line marks the regression line in pAD patients, the solid line the regression line for HC subjects.

inconclusive: (i) in the connection from the right MFG to the right SPG pAD patients showed a similar, although weaker, pattern like HC subjects (correlation with pC coefficients at a "higher" frequency band), (ii) in other fronto-cingulo-parietal connections, regression coefficients differed significantly from those of the HC subjects. In line with our hypotheses, we found significantly different relations in fronto-parietal connections. This finding reflected the results from the group comparisons, reported in earlier studies [Neufang et al., 2011; Sorg et al., 2007]. However, in contrast to our hypothesis of a preserved cingulate-associated connectivity, we did find reductions also between fronto-cingulo connections. This is also in contrast to studies reporting changes in the cingulate being associated rather with age than AD pathology [Raji et al., 2009]. However, as the cingulate was affected via fronto-cingulo connections, it might rather be due to frontal disconnection, reported by Perry and Hodges [1999] than an impaired integration of the cingulate cortex itself.

The limitations of this study are that our findings remain on the descriptive level, which means that assumptions of basic mechanisms, leading to a disruption between RSNs and task-induced connectivity patterns in early AD, remains speculative. Candidates for these pathological processes are, for example pathology-induced alterations in rs-frequency bands. For example, Garrity et al. [2007] reported heightened frequencies within the DMN in schizophrenic patients compared to HC subjects, and Stam et al. [2005] reported reduced synchronicity in AD patients during rs-EEG in the alpha band (10–13 Hz) and beta

band (13–30 Hz). Alternatively, network integration weakened due to morphometrical alterations. In an earlier study, we could show that effective connectivity declined in function of regional gray matter volume [Neufang et al., 2011; Sorg et al., 2007]. Likewise, studies combining fMRI and FDG-PET reported impaired RSN connectivity in areas of high amyloid deposition in healthy elderly [Drzezga et al., 2011; Sperling et al., 2009] as well as AD patients [Sheline et al., 2010]. Thus, it might be that AD-related changes in the brain tissue might have something to do with the disrupted relation between functional connectivity and effective connectivity.

In summary, we report findings with regard to the relation between two different modalities of cerebral connectivity. We demonstrated that they were related in healthy subject, but impaired in pAD patients. Furthermore, connectivity parameters were frequency-specific, hinting towards a crucial role of frequencies in the study of networks.

ACKNOWLEDGMENTS

The authors thank the reviewers for constructive suggestions. This work is supported by the German Federal Ministry of Education and Research (BMBF) grant 01EV0710 (AMW) and SN is supported by the Kommission für Klinische Forschung of the university hospital Klinikum Rechts der Isar, grant C21-09 / 8762753. VR is supported by the Alzheimer Forschung Initiative (AFI) grant 08860 and by the KKF grant 8762754.

REFERENCES

Achard S, Salvador R, Whitcher B, Suckling J, Bullmore E (2006): A resilient, low-frequency, small-world human brain functional network with highly connected association cortical hubs. J Neurosci 26:63–72.

Aertsen A, Preißl H (1999): Dynamics of activity and connectivity in physiological neuronal networks. In: HGS, editor. Nonlinear Dynamics and Neuronal Networks. New York: VCH Publishers. pp281–302.

Benjamini Y, Hochberg Y (1995): Controlling the false discovery rate: A practical and powerful approach to multiple testing. J Roy Stat Soc 57:289–300.

Biswal B, Van Kylen J, Hyde JS (1997): Simultanous assessment of flow and BOLD signals in resting-state functional connectivity maps. NMR Biomed 10:165–170.

Calhoun VD, Adali T, McGinty VB, Pekar JJ, Watson TD, Pearlson GD (2001): fMRI activation in a visual-perception task: Network of areas detected using the general linear model and independent components analysis. Neuroimage 14:1080–1088.

Damoiseaux JS, Greicius MD (2009): Greater than the sum of its parts: a review of studies combining structural connectivity and resting-state functional connectivity. Brain Struct Funct 213:525–533.

Drzezga A, Becker JA, Van Dijk KR, Sreenivasan A, Talukdar T, Sullivan C, Schultz AP, Sepulcre J, Putcha D, Greve D, Johnson KA, Sperling RA (2011): Neuronal dysfunction and disconnection of cortical hubs in non-demented subjects with elevated amyloid burden. Brain 134:1635–1646.

Fan J, McCandliss BD, Fossella J, Flombaum JI, Posner MI (2005): The activation of attentional networks. Neuroimage 26:471–479.

Fox MD, Zhang D, Snyder AZ, Raichle ME (2009): The global signal and observed anticorrelated resting state brain networks. J Neurophysiol 101:3270–3283.

Fox MD, Snyder AZ, Barch DM, Gusnard DA, Raichle ME (2005): Transient BOLD responses at block transitions. Neuroimage 28:956–966.

Friston KJ (1994): Functional and effective connectivity in neuroimaging: A synthesis. Human Brain Mapp 2:56–78.

Garrity AG, Pearlson GD, McKiernan K, Lloyd D, Kiehl KA, Calhoun VD (2007): Aberrant "default mode" functional connectivity in schizophrenia. Am J Psychiatry 164:450–457.

Gauthier S, Reisberg B, Zaudig M, Petersen RC, Ritchie K, Broich K, Belleville S, Brodaty H, Bennett D, Chertkow H, Cummings JL, de Leon M, Feldman H, Ganguli M, Hampel H, Scheltens P, Tierney MC, Whitehouse P, Winblad B; International Psychogeriatric Association Expert Conference on mild cognitive impairment (2006): Mild cognitive impairment. Lancet 367: 1262–1270.

Greicius MD, Supekar K, Menon V, Dougherty RF (2009): Resting-state functional connectivity reflects structural connectivity in the default mode network. Cereb Cortex 19:72–78.

Ginestet CE, Simmons A (2011): Statistical parametric network analysis of functional connectivity dynamics during a working memory task. Neuroimage 55:688–704.

Havlicek M, Friston KJ, Jan J, Brazdil M, Calhoun VD (2011): Dynamic modeling of neuronal responses in fMRI using cubature Kalman filtering. Neuroimage 56:2109–2128.

Jenkins GM, Watts, DG. 1998. Spectral analysis and its applications. Boca Raton: Emerson-Adams Press. 525 p.

Kaminski M (2007): Multichannel data analysis in biomedical research. In: Jirsa VK, McINtosh AR, editors. Handbook of Brain Connectivity. Heidelberg: Springer Verlag. pp327–356.

Lagioia A, Van De Ville D, Debbané M, Lazeyras F, Eliez S (2010): Adolescent resting state networks and their associations with schizotypal trait expression. Front Syst Neurosci 5:35.

Liao W, Mantini D, Zhang Z, Pan Z, Ding J, Gong Q, Yang Y, Chen H (2010): Evaluating the effective connectivity of resting state networks using conditional Granger causality. Biol Cybern 102:57–69.

McKhann G, Drachman D, Folstein M, Katzman R, Price D, Stadlan EM (1984): Clinical diagnosis of Alzheimer's disease: report of the NINCDS-ADRDA work group under the auspices of Department of Health and Human Services Task Force in Alzheimer's Disease. Neurology 34:939–944.

Mori S, Zhang J (2006): Principles of diffusion tensor imaging and its applications to basic neuroscience research. Neuron 51:527–539.

Morris JC, Heyman A, Mohs RC, Hughes JP, van Belle G, Fillenbaum G, Mellits ED, Clark C (1989): The consortium to establish a registry for Alzheimer's disease (CERAD). I. Clinical and neuropsychological assessment of Alzheimer's disease. Neurology 39:1159–1165.

Neufang S, Akhrif A, Riedl V, Förstl H, Kurz A, Zimmer C, Sorg C, Wohlschläger AM (2011): Disconnection of frontal and parietal areas contributes to impaired attention in very early Alzheimer's disease. J Alzheimers Dis 25:309–321.

Niazy RK, Xie J, Miller K, Beckmann CF, Smith SM (2011): Spectral characteristics of resting state networks. Prog Brain Res 193:259–276.

Ozaki TJ (2011): Frontal-to-parietal top-down causal streams along the dorsal attention network exclusively mediate voluntary orienting of attention. PLoS One 6:e20079.

Perry RJ, Hodges JR (1999): Attention and executive deficits in Alzheimer's disease. A critical review. Brain 122:383–404.

Raji CA, Lopez OL, Kuller LH, Carmichael OT, Becker JT (2009): Age, Alzheimer disease, and brain structure. Neurology 73:1899–1905.

Rossi AF, Pessoa L, Desimone R, Ungerleider LG (2009): The prefrontal contrex and executive control of attention. Exp Brain Res 192:489–497.

Salvador R, Suckling J, Schwarzbauer C, Bullmore E (2005): Undirected graphs of frequency-dependent functional connectivity in whole brain networks. Philos Trans R Soc Lond B Biol Sci 360:937–946.

Salvador R, Martínez A, Pomarol-Clotet E, Gomar J, Vila F, Sarró S, Capdevila A, Bullmore E (2008): A simple view of the brain through a frequency-specific functional connectivity measure. Neuroimage 39:279–289.

Sato JR, Takahashi DY, Arcuri SM, Sameshima K, Morettin PA, Baccalá LA (2009): Frequency domain connectivity identification: an application of partial directed coherence in fMRI. Hum Brain Mapp 30:452–461.

Sheline YI, Morris JC, Snyder AZ, Price JL, Yan Z, D'Angelo G, Liu C, Dixit S, Benzinger T, Fagan A, Goate A, Mintun MA (2010): APOE4 allele disrupts resting state fMRI connectivity in the absence of amyloid plaques or decreased CSF Aβ42. J Neurosci 30:17035–17040.

Skudlarski P, Jagannathan K, Calhoun VD, Hampson M, Skudlarska BA, Pearlson G (2008). Measuring brain connectivity: diffusion tensor imaging validates resting state temporal correlations. Neuroimage 43:554–561.

Smyser CD, Inder TE, Shimony JS, Hill JE, Degnan AJ, Snyder AZ, Neil JJ (2010): Longitudinal analysis of neural network development in preterm infants. Cereb Cortex 20:2852–2862.

Sorg C, Riedl V, Mühlau M, Calhoun VD, Eichele T, Laer L, Drzezga A, Förstl H, Kurz A, Zimmer C, Wohlschläger AM (2007): Selective changes of resting-state networks in individuals at risk for Alzheimer's disease. Proc Natl Acad Sci USA 104:18760–18765.

Sperling RA, Laviolette PS, O'Keefe K, O'Brien J, Rentz DM, Pihlajamaki M, Marshall G, Hyman BT, Selkoe DJ, Hedden T, Buckner RL, Becker JA, Johnson KA (2009): Amyloid deposition is associated with impaired default network function in older persons without dementia. Neuron 63:178–188.

Stam CJ, Montez T, Jones BF, Rombouts SA, van der Made Y, Pijnenburg YA, Scheltens P (2005): Disturbed fluctuations of resting state EEG synchronization in Alzheimer's disease. Clin Neurophysiol 116:708–715.

Stephan KE, Friston KJ (2010): Analyzing effective connectivity with fMRI. Wiley Interdiscip Rev Cogn Sci 1:446–459.

Stephan KE, Friston KJ, Frith CD (2009): Dysconnection in schizophrenia: from abnormal synaptic plasticity to failures of self-monitoring. Schizophr Bull 35:509–527.

Sun FT, Miller LM, D'Esposito M (2004): Measuring interregional functional connectivity using coherence and partial coherence analyses of fMRI data. Neuroimage 21:647–658.

Supekar K, Musen M, Menon V (2009): Development of large-scale functional brain networks in children. PLoS Bio 7:e1000157.

Supekar K, Menon V, Rubin D, Musen M, Greicius MD (2008): Network analysis of intrinsic functional brain connectivity in Alzheimer's disease. PLoS Comput Biol 4:e1000100.

Van den Heuvel MP, Hulshoff Pol HE (2010): Exploring the brain network: a review on resting-state fMRI functional connectivity. Eur Neuropsychopharmacol 20:519–534.

Van Dijk KRA, Hedden T, Venkataraman A, Evans KC, Lazar SW, Buckner RL (2010): Intrinsic functional connectivity as a tool for human connectomics: Theory, properties, and optimization. J Neurophysiol 103:297–321.

Wang L, Zang Y, He Y, Liang M, Zhang X, Tian L, Wu T, Jiang T, Li K (2006): Changes in hippocampal connectivity in the early stages of Alzheimer's disease: Evidence from a resting state fMRI. NeuroImage 31:496–504.

Wee CY, Yap PT, Zhang D, Denny K, Browndyke JN, Potter GG, Welsh-Bohmer KA, Wang L, Shen D (2011): Identification of MCI individuals using structural and functional connectivity networks. Neuroimage 59:2045–2056.

Ystad M, Hodneland E, Adolfsdottir S, Haász J, Lundervold AJ, Eichele T, Lundervold A (2011): Cortico-striatal connectivity and cognition in normal aging: A combined DTI and resting state fMRI study. Neuroimage 55:24–31.